

## Olivine-Bearing Rocks of the Lapland Granulite Belt (Baltic Shield)

E. N. Terekhov\*, T. F. Shcherbakova, and A. N. Konilov

*Geological Institute, Russian Academy of Sciences, Pyzhevskii per. 7, Moscow, 119017 Russia*

\**e-mail: tereh@ilran.ru*

Received September 28, 2015; accepted November 12, 2015

**Abstract**—Olivine-bearing varieties of garnet–clinopyroxene crystalline schists of the Lapland granulite belt have been studied in detail for the first time. Two types of olivine (iron mole fractions of 27 and 38%) are distinguished. Olivine with lower Fe content occurs as inclusions in clino- and orthopyroxene and in terms of CaO and Cr contents is close to magmatic minerals. Olivine with high Fe content presumably suffered high- and moderate-temperature metamorphism. The olivine-bearing rocks contain several grains of omphacite with 30–37 mol % jadeite and garnet with 44–50 mol % pyrope, which can be regarded as relict assemblages of the early stage of eclogitization of a magmatic protolith. The presence of symplectites indicates their retrograde transformation during decompression. The protoliths of the studied rocks could be olivine gabbro-norites and pyroxenites. It was found that the rocks contain high-alumina minerals: corundum, spinel, and sapphirine. In addition, Al<sub>2</sub>O<sub>3</sub> content in some amphibole grains is as high as 19 wt %. This indicates that the ascent of the deep-seated rocks was accompanied by interaction with Al-rich fluid. The positive Eu anomaly in the olivine-bearing rocks and some of their minerals is indicative of the reducing character of fluid. Activation of fluid reworking leading to the formation and transformation of the olivine-bearing rocks, transfer of alumina and its precipitation at different depths are related to the processes at the base of the Paleoproterozoic rift system of Karelides.

**Keywords:** granulite, eclogite, olivine, garnet, corundum, positive Eu anomaly

**DOI:** 10.1134/S001670291609010X

### INTRODUCTION

The Lapland granulite belt in the northern Baltic Shield carries information on the composition of deep lithosphere. Olivine–pyroxene–garnet rocks were recently found in its eastern part (Fonarev et al., 2007). In this paper, we described in detail these rare rocks to gain a better understanding of the formation of the deep-seated portions of the Earth's crust and granulite belts.

### GEOLOGICAL POSITION AND RELATIONS OF ROCKS

The studied olivine-bearing metamorphic rocks were found in the Kandalaksha–Kolvitsa massif, which represents the fragment of the Lapland granulite belt. Granulites gently rest on granite gneisses. Reverse metamorphic zoning indicates their overthrust relations, the nature of which remains unclear. According to (Marker, 1985, Kozlov et al., 1990), granulites are volcanosedimentary rocks that were metamorphosed and exhumed to the surface in a compression setting. Terekhov (2007) believes alternatively that the granulites and entire Lapland–Belomorian belt in the Early Paleoproterozoic served as a deep-seated “pillow” in the rift system of Karelides. The latter, in turn, were formed by two pulses of magmatic

activity (2.45–2.4 and 2.1–1.95 Ga), which predetermined defragmentation of Archean crust and formation of comagmatic rocks at different depths: anorthosites (at a depth of 50–45 km), drusites (30–20 km), layered intrusions (15–3 km), and volcanic rocks (Mitrofanov and Nerovich, 2003). The Lapland belt is characterized by tectonic layering: garnet amphibolites–metaanorthosites–garnet–clinopyroxene rocks–mafic and felsic granulites. The basal part of the Lapland granulite nappe is interpreted as a ductile shear zone made up of garnet amphibolites–tectonites after different protoliths (Terekhov and Levitsky, 1993). Similar boundaries of granulite complexes with granite–gneiss are found widely around the world (Perchuk et al., 2002). The boundary is marked by alkali granites formed at the final stage of nappe formation. However, these granites are ascribed to A-type granites generated in an extensional setting (Terekhov and Efremova, 2005), which is inconsistent with collisional models of the Lapland nappes (Mints et al., 1996). No age data are available on the rocks of the Kandalaksha structure, but many determinations were obtained for compositionally similar Kolvitsa gabbro-anorthosite massif in the adjacent structure. The timing of magmatic crystallization and the first stage of metamorphism of this massif is estimated at 2.45 Ga (Frisch et al., 1995). Magmatic crystallization and

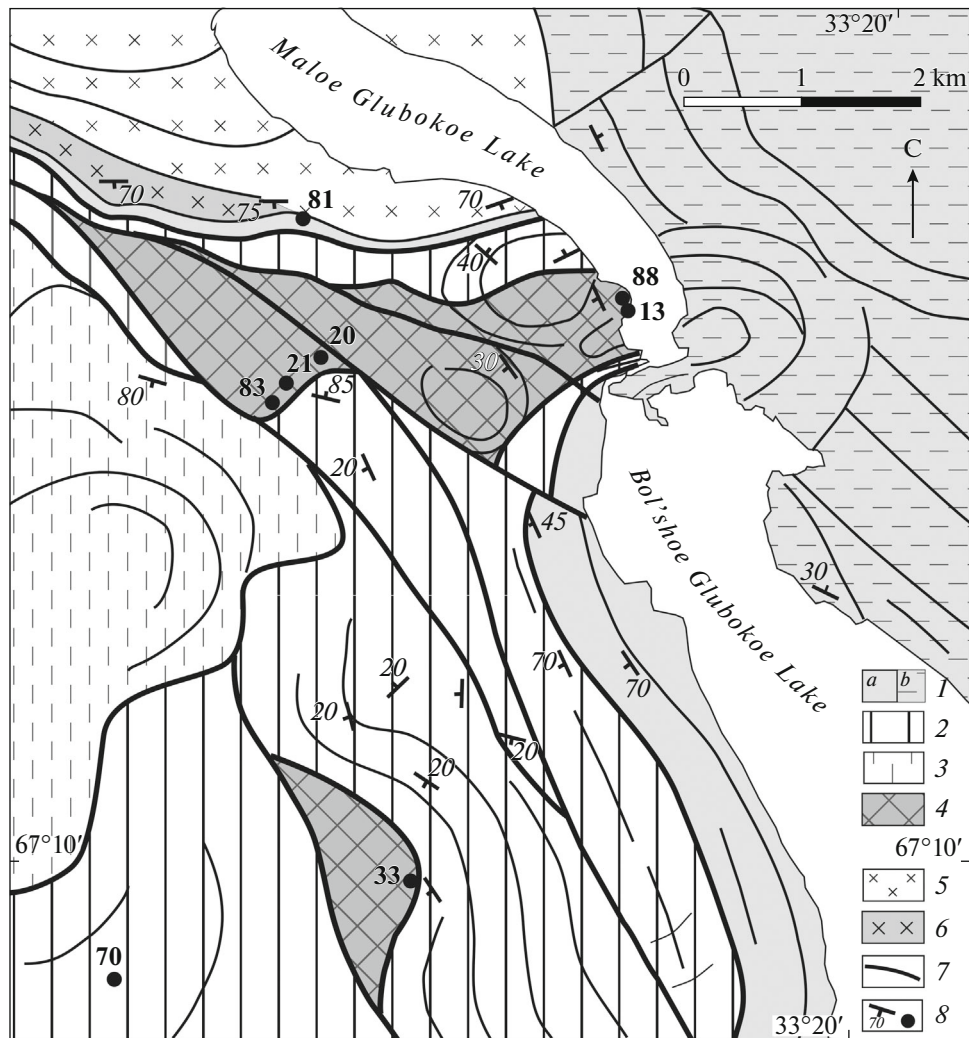


**Fig 1.** Geological position of the olivine-bearing rocks in the eastern part of the Kandalaksha structure. 1—garnet amphibolites: without relicts (a) and with relicts of mafic granulites (b); 2—gabbroanorthosites; 3—garnet—clinopyroxene rocks; 4—the same, with bodies of the olivine-bearing rocks, mafic and felsic granulites; 5—Belomorian Complex; 6—alkali granites; 7—faults; 8—dip and strike and sampling localities.

subsequent metamorphism occurred under a pressure of 12–13 kb (Fonarev, 2004). Then, the rocks were brought to the ductile–brittle boundary, where they formed protrusions among the rocks of the Belomorian Complex. During 1.8–1.7 Ga, the granulites together with the Belomorian Complex were exhumed to the surface as a metamorphic core, which at present forms the Lapland–Belomorian belt (Terekhov, 2007).

The olivine-bearing varieties are more massive rocks than surrounding *Grt*–*Cpx* rocks. They compose lenticular bodies from 0.2 to 3 m thick and from tens to few hundreds of meters long, which have vague contacts and are practically indistinguishable from the host rocks. They were found in the eastern part of the Kandalaksha synform (Fig. 1), in association with mafic granulites (*Grt*–*Opx*–*Cpx*–*Pl* rocks) and linear zones of felsic granulites. Similar sequence is known in the Por'ya Guba area. The mafic granulites in this area

are replaced by 2.5-Ga old enderbites (Kaulina and Bogdanova, 2000), which allows us to consider them as a framework for gabbroanorthosite intrusions. The locality of the olivine-bearing rocks in the Kandalaksha synform is characterized by steep dipping of rocks and the presence of ring structures, which are not typical of other parts of the belt. In terms of some features, it may be regarded as the root part of the massif thrust over the granite-gneiss complex, while the olivine-bearing rocks may be considered as fragments of dikes or zones of fluid reworking.

## METHODS

Major oxide composition was determined at the Vinogradov Institute of Geochemistry, Siberian Branch, Russian Academy of Sciences, in Irkutsk, while trace and rare-earth elements were analyzed at

the Institute of Lithosphere of the Russian Academy of Sciences by XRF method on a TEFA-III analyzer, by atomic absorption on a "Perkin-Elmer 5000" spectrophotometer, and by ICP-MS at the Institute of Mineralogy, Geochemistry, and Crystal Chemistry of the Rare Elements. Compositions of minerals were analyzed on a "Camebax" microprobe equipped with EDS "Link-860" at the Institute of Experimental Mineralogy of the Russian Academy of Sciences, Chernogolovka. Of over 50 analyzed samples, data on six olivine-bearing and three olivine-free samples were used in this work. In each sample, we analyzed 20–45 grains of different minerals, including rims and cores of definite minerals, as well as minerals in symplectites.

### PETROGEOCHEMISTRY OF THE OLIVINE-BEARING ROCKS

During study of *Grt-Cpx* rocks of the Kandalaksha structure, olivine was identified in six samples. The finds of this mineral are very unusual of the Lapland granulite belt. In terms of mineral and chemical composition, three samples (20.3, 21.1, 83.2) correspond to ultramafic rocks, and three samples (13.3, 33.3, 88.1) are mafic rocks. The ultramafic varieties as compared to mafic rocks are two–three times higher in MgO, but have lower contents of alkalis and calcium (Table 1).

**The olivine-bearing rocks of ultramafic composition (type I).** Major minerals are represented by *Cpx* (50–60%) and *Grt* (30–35%). *Ol* content varies from single grains to 10%, *Opx* accounts for up to 5%. Bright brown amphibole and ore mineral account for around 1%. Amphibole is grouped into thin discontinuous subparallel bands. Biotite forms aggregates of fine plates with inclusions of *Grt* and *Cpx*, sometimes, with serpentine (Fig. 2a). The rocks have heterogeneous structure. Less deformed rocks are fine-grained, with thin-banded structure. *Cpx* forms light green isometric and prismatic grains around 1mm in size. *Opx* is observed as irregular grains or plates up to 1.4 mm long. *Grt* is present as fine (less than 0.1 mm), tightly adjoined grains forming aggregates as bands up to 6 mm in size and patches up to  $3.7 \times 2.5$  mm (Fig. 2e).

**The olivine-bearing rocks of mafic composition (type II).** The rocks of this type are close to rocks of type I, but differ in the presence of 5 to 20% *Pl*. Predominant minerals are *Cpx* and *Grt* (40–50% and 25–5%); *Ol* accounts for 3–5%. *Opx* is observed as single individual grains and in symplectites with *Cpx* and *Pl* (Figs. 3 and 4). In rocks of this type, small *Grt* grains are arranged around *Cpx* and *Pl* to form rims (coronas). Accumulations with relicts of *Cpx* and *Pl* are less common. *Grt* also forms chains along cleavage planes of *Pl*.

Olivine in the rocks of types I and II varies from 3 to 10%, but is poorly distinguishable in deformed varieties. It is usually represented by small (0.2–0.4 mm) isometric grains with rounded or finely uneven out-

lines. There are also large ( $0.7 \times 0.6$  mm) grains (Fig. 3a). Sometimes, olivine has a rhombohedral shape with smoothed edges. In sample 88.1, olivine grain is enclosed in *Cpx*. The outlines of *Cpx* and *Ol* are uneven. *Cpx* is surrounded by aggregate of finely brecciated grains, which indicates rock deformation (Fig. 2c). In sample 21.1, *Ol* is localized closely to reticulate serpentine saturated in ore dust (Fig. 2a). Very small *Ol* inclusions were found in *Cpx* (Figs. 2a, 2b) and *Opx* (Figs. 3b, 3d).

### Composition of Minerals

**Olivine.** Analysis of 25 grains allowed us to distinguish two varieties. Olivine from type I rocks with higher MgO content is dominated by forsterite component, with Fe mole fraction of 27–28%. Olivine in type-II rocks ( $\text{FeO} > \text{MgO}$ ) has higher content of fayalite component (35–39%). Fe-rich olivines have higher chromium content, but lower Mn content and almost always contain Ti, which is completely absent in Mg-rich olivines (Table 2). Fine *Ol* inclusions in *Cpx* have the higher Mg composition of 82% ( $X_{\text{Mg}} = \text{Mg}/(\text{Mg} + \text{Fe})\%$ ). Olivine in orthopyroxene is characterized by Mg number of 74–76%. Composition of some *Ol* grains is correlated with that of associated *Grt*. In particular, Fe-rich *Ol* (points 41–43, sample 13.3) is in contact with high-Fe ( $X_{\text{Fe}} = 61\%$ ) garnet, which contains 52 mol % almandine (point 39, Fig. 4a), but low pyrope content (34 mol %). High-Mg *Ol* (point 4, sample 21.1) is in contact with garnet *Grt* (point 5) with low Fe mole fraction and lower almandine content of 38 mol %, but much higher pyrope content of 48.5 mol. % (Fig. 2b).

**Orthopyroxene** in different grains have close proportions of major components. The  $\text{Al}_2\text{O}_3$  content in most grains is 1–2 wt % and only one grain contains 4.2 wt%. In some *Opx* cores are enriched in  $\text{Al}_2\text{O}_3$  and  $\text{TiO}_2$  relative to rims. The  $\text{Cr}_2\text{O}_3$  content usually accounts for less than 1 wt %, reaching 1.83 wt % only in one grain, which possibly represents a relict of magmatic mineral. *Opx* in symplectites has lower Mg, but higher Fe and Mn contents. Orthopyroxenes intergrown with *Cpx* (points 7–6 and 24–25) (Figs. 4b, 4d) and plagioclase (points 18–17) (Fig. 4c) have similar compositions.

Clinopyroxene from type I rocks contains 2.53–5.44 wt %  $\text{Al}_2\text{O}_3$  and 1.75–3.14 wt %  $\text{Na}_2\text{O}$ . The jadeite end member varies from 7.6 to 23.1 mol % (Fig. 5a). Clinopyroxene from type II rocks has somewhat different composition. It shows higher  $\text{Al}_2\text{O}_3$  (4.01–7.23 wt %, reaching 8.97–12.41 wt % in some samples),  $\text{Na}_2\text{O}$  (2.80–5.33 wt %), and jadeite (18.2–36.9 mol %). In both rock types, *Cpx* is heterogeneous in composition and differs within one sample (Fig. 5a). It usually reveals a prograde zoning, with rims higher in jadeite (by 5–11 mol %) than cores. In two grains from sample 13.3, this difference is 14 and 16 mol %:

**Table 1.** Representative analyses and mineral composition of olivine-bearing and associated rocks (wt %, ppm)

Component	1	2	3	4	5	6	7	8	9
	21.1	83.2	88.1	13.3	33.3	83.1	13.1	70.1	81.1
SiO <sub>2</sub>	40.32	41.51	44.78	46.04	48.36	45.57	47.31	49.63	53.28
TiO <sub>2</sub>	0.12	0.23	0.22	0.20	0.77	1.82	0.48	0.50	1.98
Al <sub>2</sub> O <sub>3</sub>	8.67	11.64	15.14	18.01	17.81	18.98	19.25	26.55	11.80
FeO <sub>tot</sub>	18.43	21.16	17.94	14.34	13.73	14.81	12.23	5.04	18.66
MnO	0.21	0.25	0.20	0.16	0.18	0.15	0.14	0.08	0.32
MgO	24.04	17.37	13.74	10.81	6.94	5.74	8.23	1.50	2.63
CaO	4.87	7.11	6.82	8.01	9.58	10.19	9.10	12.97	7.66
Na <sub>2</sub> O	0.65	1.20	1.48	2.05	2.36	2.59	2.73	3.05	1.36
K <sub>2</sub> O	0.14	0.09	0.26	0.29	0.18	0.13	0.42	0.33	1.70
P <sub>2</sub> O <sub>5</sub>	0.03	0.04	0.05	0.04	0.11	0.06	0.06	0.12	0.61
L.O.I.	2.43	0.20	0.51	0.06	0.11	0.04	0.13	0.16	0.44
Cr	100	39	38	—	156	57	—	—	—
Ni	94	610	410	407	163	96	308	15	46
Co	160	140	107	—	—	49	—	—	—
V	30	45	45	—	—	320	—	—	—
Rb	4.1	2	1	2	2	3	5	14	41
Ba	63	42	66	99	128	67	105	—	459
Sr	122	120	170	185	262	327	212	—	70
Zr	12	42	49	36	31	36	52	14	293
Y	2.6	2	8	4	11	8	13	8	81
La	2.3	2.1	4.2	3.7	6.7	3.6	6	8.6	29
Ce	4.8	2.7	6.6	3.7	8.7	6.6	8.8	19	79
Nd	2.3	2.4	2.0	5.6	7.8	3.2	6.5	8	41
Sm	0.48	1.00	2.00	1.90	2.3	1.20	1.90	0.90	10.00
Eu	0.20	0.28	0.50	0.60	1.1	0.73	0.80	1.30	3.00
Gd	0.46	0.73	0.60	0.80	1.3	1.00	1.20	1.80	11.00
Er	0.31	0.46	0.60	0.50	1.1	1.10	0.80	0.90	7.00
Yb	0.33	0.16	0.30	0.22	0.82	0.43	0.34	0.70	5.40
(La/Yb) <sub>n</sub>	4.7	8.7	9.3	11.2	6	5.7	12	8.8	3.6
F, %	43.4	54.6	56.3	56.6	66.5	74.4	60.1	77.1	68.1
Olivine	X	X	X	X	X	—	—	—	—
Orthopyroxene	X	X	X	X	X	—	X	—	—
Clinopyroxene	X	X	X	X	X	X	X	X	X
Garnet	X	X	X	X	X	X	X	X	X
Plagioclase	—	—	X	X	X	X	X	X	X
Amphibole	X	X	X	—	—	X	X	X	X
Spinel	—	—	X	X	X	—	X	—	—
Sapphirine	—	—	X	—	—	—	—	—	—
Corundum	—	—	—	—	X	—	X	—	—

(1–5) olivine-bearing rocks; (6–7) garnet–clinopyroxene crystalline schists; (8) metaanorthosite; (9) garnet amphibolite. X—mineral is present.



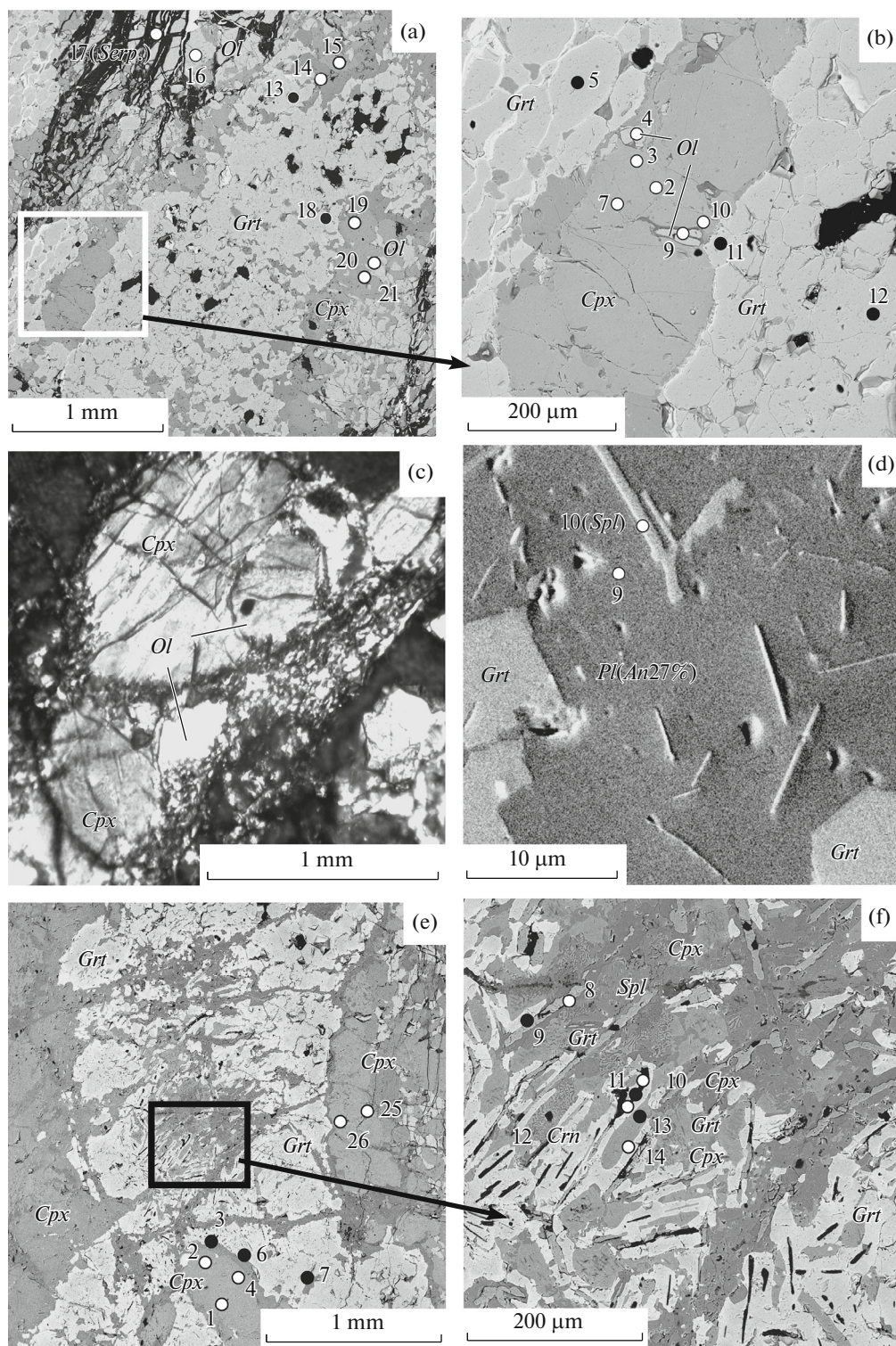


**Fig. 2.** Microimage of the olivine-bearing (samples 21.1 (a and b) and 88.1 (c and d)) and *Grt-Cpx* ultramafic rocks (sample 20.3 (e and f)). (a)—sheared rock: its large grains and serpentine (dark in the top left corner) are elongated in the same direction. (a) Fine *Ol* inclusions in *Cpx*, points 16 and 20; (b) fine *Ol* grains: points 4 and 9 in *Cpx* with 16% jadeite are in contact with *Grt* grains (points 5, 11) with 43.7 and 48.5 mol % pyrope; (c) zone of brecciated olivine-bearing rock with *Cpx* “eye” and *Ol* inclusion. Crossed nicols; (d) spinel lamellae in plagioclase; (e) part of the band formed by *Crtn*, *Grt* (points 3, 7) have weak reverse zoning, like *Cpx* in points 25, 26; (f) —*Grt* (points 9, 11, 13)—*Cpx* (points 10, 14) symplectite with lamellae of spinel (point 8—light) and corundum (point 12—dark). *Cpx* from points 10 and 14 has the highest  $Al_2O_3$ —13.86 and 14.48%, respectively. Hereinafter, black circles show the analyzed (*Grt*), light circles, all other minerals: olivine (*Ol*), orthopyroxene (*Opx*), clinopyroxene (*Cpx*), plagioclase (*Pl*), spinel (*Spl*), serpentine (*Serp*), hornblende (*Hb*), corundum (*Crn*), biotite (*Bt*).



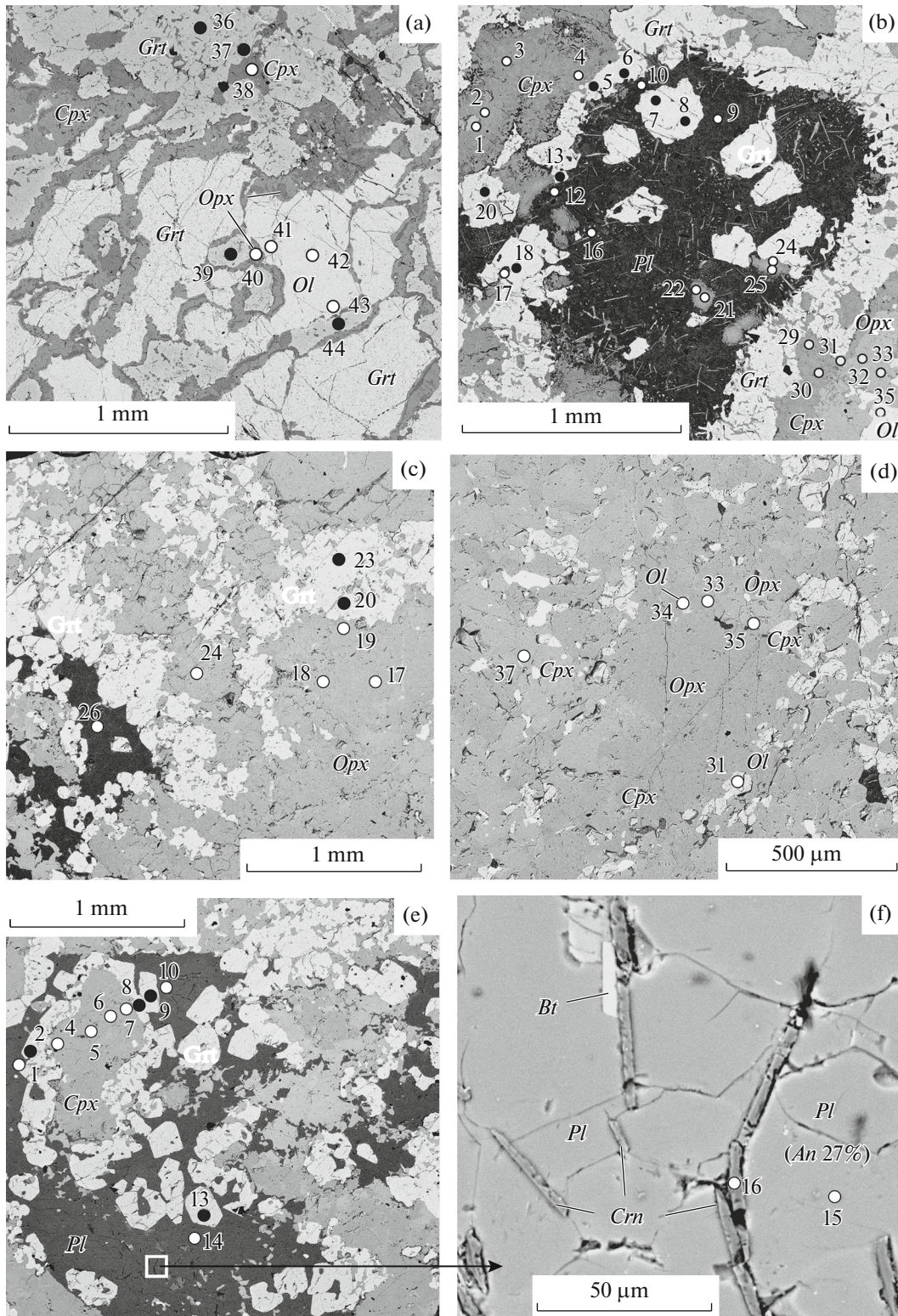


**Fig. 3.** Microimage of type-II olivine-bearing rocks: samples 13.3 (a and b) and 33.3 (c–f) (a) *Ol* grain (points 41–43) in contact with *Opx* (point 40) and *Grt* (points 39, 44: pyrope 33.6 and 34.8 mol %); (b) *Pl* with grains of *Grt* and relicts of omphacite (points 21, 22 and 24, 25), surrounded by *Grt* rim (pyrope 26–29 mol %), one grain (point 17) contains omphacite inclusion (point 18, jadeite 36.9% with high  $Al_2O_3$  – 13.18%); (c) unzoned *Grt* (pyrope 42 mol %) among grains of homogenous *Opx*, dark—chains of sodic *Pl* (An 18.5 mol %); (d) small inclusions of *Ol* (points 31, 34) in *Opx*; (e) *Grt* rims around *Cpx* and *Pl*, *Cpx* of complex composition (points 4–7), one of the rim is jadeite 27 mol %, *Grt* is unzoned, contains 44.8 mol % pyrope, i.e., compositions of *Cpx* and *Grt* in this domain are close to those of eclogite; (f) oriented corundum crystals with visible axial zone in plagioclase.



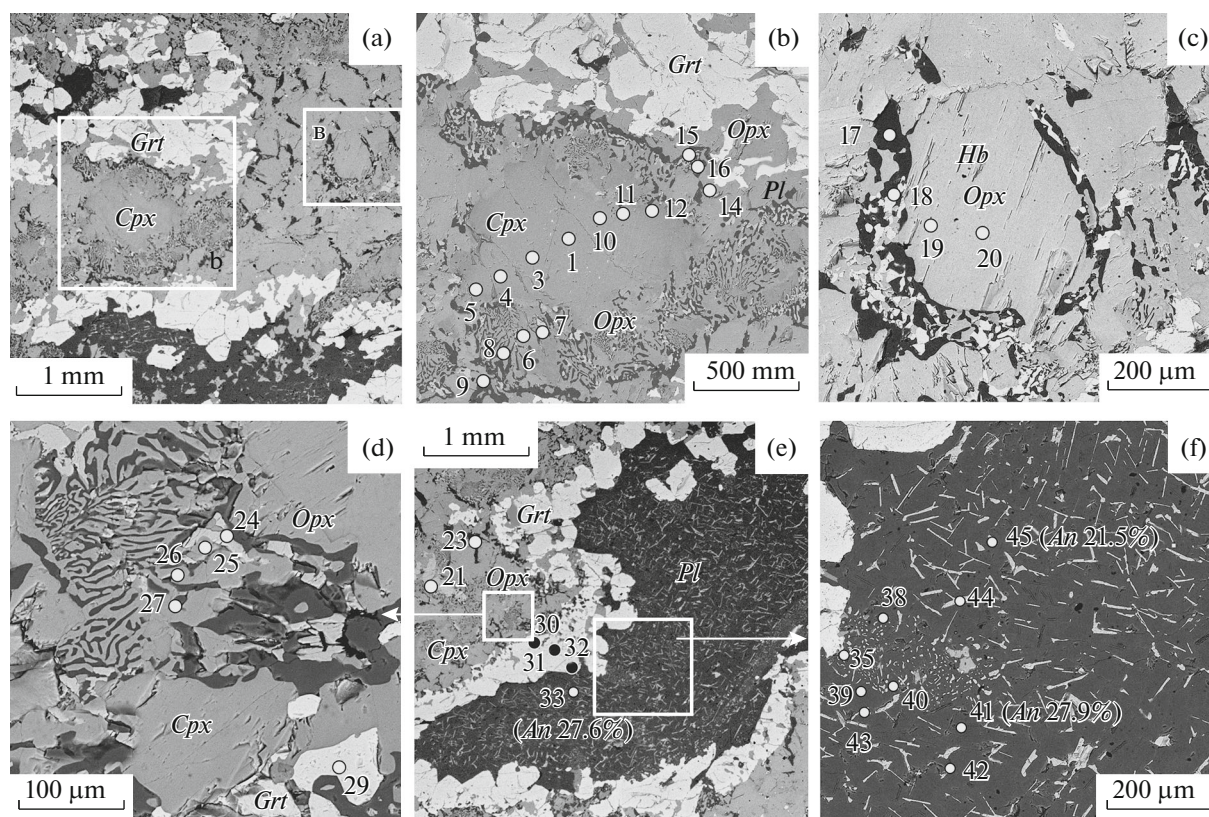


**Fig. 4.** Microimage of the olivine-bearing rock (sample 13.1) (a) symplectitic Cpx with *Grt* rim; (b) *Cpx* symplectite (point 6) with *Opx* (point 7), and (point 8) with *Pl* (point 9); (c) amphibole (points 19, 20) among *Opx* (points 18)—*Pl* (point 17) symplectite; (d) *Opx* (point 24)—*Cpx* (point 25, jadeite 5.7 mol %) and *Cpx* (point 26, jadeite 6.0 mol %)—*Pl* (point 27, An 21.6 mol %) symplectites; (e) *Pl* prism (An 27.6%) bent during rock deformation, with *Grt* rim; (f) *Pl* (points 41 and 45) with spinel lamellae.

33.7 and 36.10 mol % jadeite in rims. Both these grains are small, with uneven margins, and are enclosed in plagioclase An 35 mol %. Individual grains show complex zoning. In particular, the profile across *Cpx* (points 4–7) in sample 33.3 (Fig. 3e) shows the following variations in jadeite content: 27.0, 20.5, 23.1, 25.5 mol %. Thus, one zones are close to omphacite, while others, to diopside. This *Cpx* is surrounded by *Grt* rim with pyrope content of 44.0 and 44.8 mol % (points 8, 9, Fig. 3e). In *Cpx* from symplectites, jadeite varies from 14 to 1.8 mol %, which is 8–10 mol % lower than in individual grains. The lowest jadeite content (1.8 mol %) was found in *Cpx* (point 23, sample 20.3) from symplectite with hornblende. *Cpx* in symplectite with *Grt* (Fig. 2f, sample 20.3) has the highest  $\text{Al}_2\text{O}_3$  contents (13.86–14.48 wt % – points 10, 14), but is depleted in  $\text{Na}_2\text{O}$  (2.14 and 1.44 wt %) and jadeite (15 and 10 mol %, respectively). *Grt* in this symplectite (points 9, 11, 13) is characterized by sufficiently high (32, 36, 33.5 mol %) content of pyrope component. It is also enriched in calcium component (35.9 mol %), but depleted (0.6 mol %) in spessartine end member. Garnet of such composition is close to the eclogitic garnet. Garnet in this symplectite contains numerous lamellae of corundum (point 12) and

spinel (point 8, Fig. 2f). We may suggest that the development of *Grt* after *Cpx* was controlled by Al-rich fluid, excess of which saturated newly formed *Cpx* and precipitated as corundum. *Cpx* grains with 28–36.9 mol % jadeite in rims and 18–23 mol % in cores are regarded as close to omphacite formed under conditions of prograde metamorphism, i.e. as relict eclogitic minerals. *Cpx* with the lower jadeite content (2.4–1.8 mol %) represents transformed omphacite. It is characterized by the lowered content of  $\text{Al}_2\text{O}_3$  and  $\text{Na}_2\text{O}$ , higher  $\text{MgO}$ , being close to diopside–salite.

We pay particulate attention to *Cpx* with 36.9 mol % jadeite, which occurs as oikocryst in *Grt* with 29.5 mol % pyrope (point 18, samples 13.3, Fig. 3b). Metamorphic conditions for eclogites from the Gridino area, Belomorian zone, were determined at 865°C and 14.5 kb using mineral pair: omphacite (jadeite 40 mol %)—garnet (pyrope 27 mol %) (Volodichev et al., 2004). The studied *Cpx* inclusion and host *Grt* are similar in composition to the mineral pair from the Gridino eclogites. We may suggest that omphacite inclusion in *Grt*, and above described omphacite in *Pl*, were formed in similar conditions comparable with *P–T* conditions of the Gridino eclogites, which correspond to the eclogite facies.

**Table 2.** Composition of olivine from the rocks of the Kandalaksha Massif

Component, wt %	Sample 21.1					Sample 83.2					
	1	4	9	16	20	14	15	24	28	29	
	Incl.	Incl.	Incl.	Core	Incl.	Rim	Core	Core	Core	Core	
SiO <sub>2</sub>	38.65	38.34	38.9	38.08	38.18	36.73	36.35	37.50	36.90	36.79	
TiO <sub>2</sub>	—	—	—	—	—	0.02	0.02	0.04	—	0.04	
Al <sub>2</sub> O <sub>3</sub>	0.06	—	—	—	—	0.03	0.03	0.08	0.05	0.09	
Cr <sub>2</sub> O <sub>3</sub>	0.04	0.06	0.06	0.05	0.09	0.12	0.12	0.06	—	0.06	
FeO	24.43	24.74	23.83	24.72	25.16	33.82	32.83	32.21	31.86	32.68	
MnO	—	0.13	0.18	0.08	0.2	0.02	0.22	0.02	0.02	0.10	
MgO	36.75	36.7	36.87	37.03	36.28	32.02	31.51	33.74	32.98	32.56	
CaO	0.06	0.03	0.14	0.01	0.09	0.03	—	0.05	—	0.02	
K <sub>2</sub> O	0.01	—	0.02	0.03	—	0.01	—	0.02	0.04	0.02	
F, %	27.20	27.40	26.60	27.20	28.00	37.20	36.90	34.90	35.10	36.50	
	← one grain →										
Component, wt %	Sample 13.3			Sample 33.3			Sample 88.1				
	41	42	43	31	34	21	23	24	27	37	35
	Rim 1	Core	Rim 2	Incl.	Incl.	Core	Core	Rim	Core	Core	Rim
SiO <sub>2</sub>	36.42	35.77	36.13	38.33	38.28	36.14	35.88	35.48	35.65	35.57	35.85
TiO <sub>2</sub>	—	—	0.11	—	—	0.01	—	—	—	—	0.03
Al <sub>2</sub> O <sub>3</sub>	0.04	—	0.22	—	—	0.19	0.06	0.03	0.03	0.11	0.07
Cr <sub>2</sub> O <sub>3</sub>	0.09	0.26	0.13	0.20	—	0.12	—	—	—	0.07	—
FeO	33.22	33.47	33.54	24.64	24.99	31.99	33.41	33.90	33.17	33.39	33.06
MnO	0.13	0.04	0.23	0.19	0.30	0.15	0.04	0.20	0.05	0.06	0.11
MgO	29.61	30.02	29.21	36.61	36.33	31.28	30.60	30.33	31.06	30.77	30.54
CaO	0.00	0.00	0.11	—	—	0.07	0.01	0.03	—	—	0.06
K <sub>2</sub> O	—	0.04	0.06	0.03	0.10	0.04	—	0.04	0.04	0.04	—
F, %	38.60	38.50	39.20	27.40	27.80	36.50	38.00	38.50	37.50	37.80	37.7
	← one grain →						← one grain →				

Samples 21.1 and 83.2 have ultramafic composition, while samples 13.3, 33.3, and 88.1 have mafic composition. Numerals in the second row from the top denote the number of measured grain; F, % = Fe/(Fe + Mg).

**Garnet.** More than half of the garnet grains show retrograde zoning and only one grain reveals prograde zoning (points 36, 37, sample 13.3). Other grains demonstrate complex zoning or are homogenous in composition. Zoning is weak: cores are only 2–7% higher in pyrope molecule. Most of the *Grt* grains contain from 33 to 43 mol % pyrope end member (Fig. 5b). In terms of calcium content, garnets are subdivided into two types. One type contains 27–35 mol % Ca end member, at less than 1 mol % spessartine and the lowered content of almandine. Such grains are likely close in composition to eclogitic garnet. Other garnets contain 38–44 mol % pyrope, only 12–15 mol % grossular, but have higher contents of spessartine and almandine. These grains likely experi-

enced retrograde transformations. Two grains (point 37, sample 20.3 and point 5, sample 21.1) differ in the highest content of pyrope molecule – 47.6 and 48.5%. These grains are associated with *Cpx* (points 35 and 7, samples 20.3 and 21.1) containing 7.7 and 16.4 mol % jadeite. This clinopyroxene contains two small *Ol* inclusions (Fig. 2b). Association of high-pyrope *Grt* and low-jadeite *Cpx* is frequently observed. Small unevenly shaped *Grt* grains were found in *Pl* (Fig. 2b). One of them (points 7, 8) has unusual composition: it opposite rims differ by 7 mol % in terms of pyrope and almandine content, while calcium and spessartine end members show almost two times difference. Grains of *Grt* and omphacite present in *Pl* were likely formed at the early stage of eclogitization, owing to the interac-



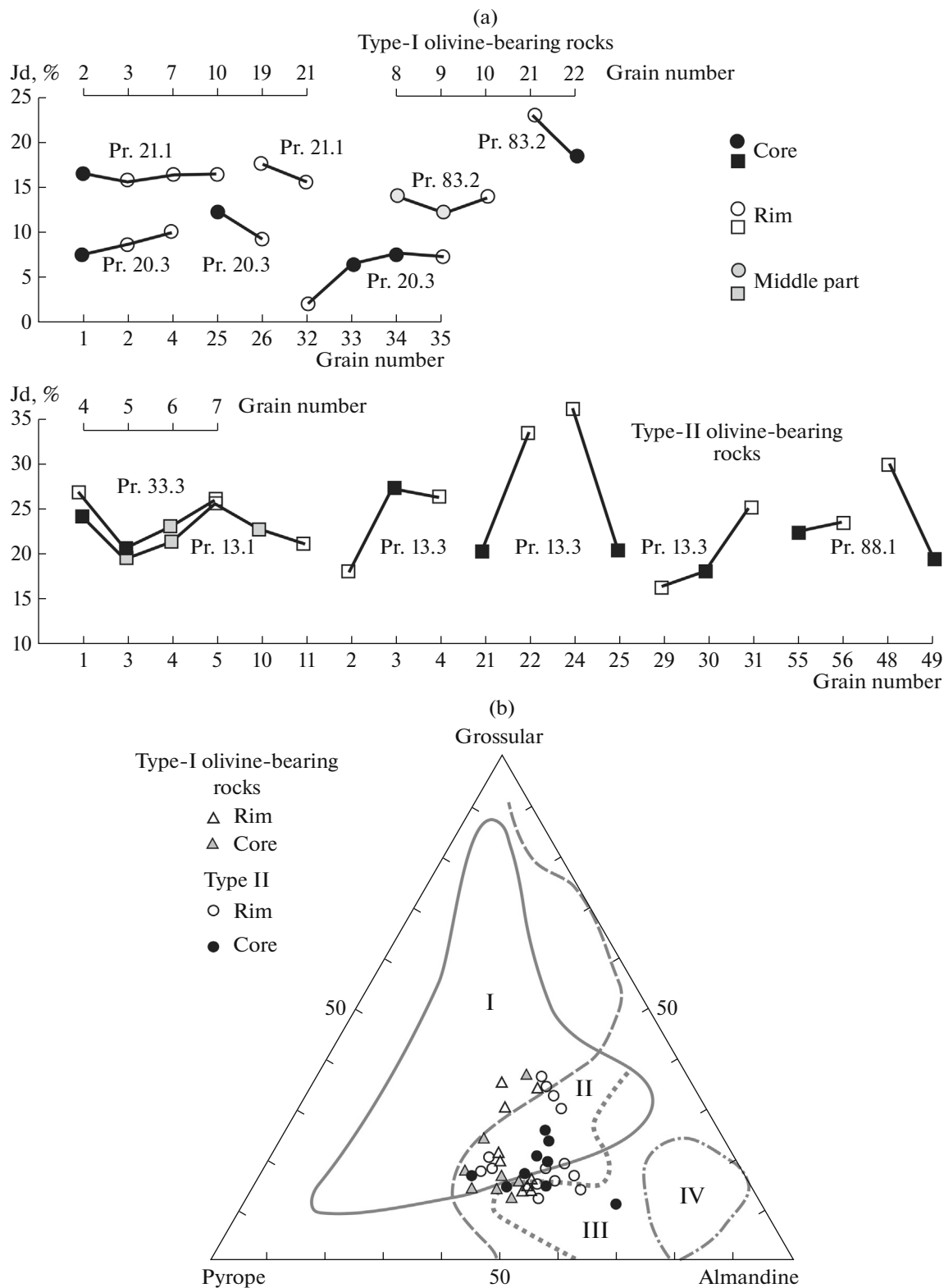


**Fig. 5.** Distribution of jadeite in clinopyroxene (a) and compositions of garnets of the studied rocks in the diagram for garnet depth facies after (Sobolev, 1963) (b). (a): numbers on horizontal axes correspond to the measurement points; (b): fields of the metamorphic facies: I—eclogite, II—granulite (together with kyanite gneiss and schist facies), III—amphibolite, IV—epidote—amphibolite.

tion between olivine and labradorite with participation of diopside. Unusual composition of *Grt* is likely related to the zoning of primary labradorite.

**Plagioclase** is present in the type II rocks. It forms three morphologies: large crystals, chains of small grains, and symplectitic intergrowths. The three varieties are different in composition. Large prisms are represented by oligoclase (An 26–28 mol %) and andesine (An 33–35 mol %). They contain numerous randomly oriented spinel lamellae, which were formed owing to the acidification of Pl, i.e. decrease of anorthite component. The composition of *Pl* in the symplectites with *Cpx* and *Opx* corresponds to the sodic oligoclase (An 22–16 mol %). Small grains localized between *Grt* or *Grt* and *Cpx* and forming chains have similar composition (points 26, 1, Figs. 3c, 3e).

**Amphibole** is observed as single grains superimposed on the early minerals, as well as in symplectite intergrowths. It is usually green, but acquires bright brown coloration in association with brown biotite in sample 13.1. These minerals contain up to 3 wt % TiO<sub>2</sub>. In some amphiboles, Al<sub>2</sub>O<sub>3</sub> content increases up to 19 wt %, accounting for 10–15 wt % in most grains. Enrichment of amphibole in Al<sub>2</sub>O<sub>3</sub> may indicate the elevated activity of this oxide at the late stages of the rock evolution.

#### High-Alumina Minerals

High-alumina minerals previously unknown in the Lapland granulite belt have been revealed in the studied rocks: corundum, spinel, and sapphirine. Corundum is observed as thin (acicular) prisms 0.1–0.5 μm wide and up to 100 μm long, which are oriented in two directions at angle of approximately 80°–90°, which approximates exsolution lamellae. It was found in *Pl* (An 27.4%) (Fig. 3f) and *Cpx*–*Grt* symplectite (Fig. 2f). Corundum contains hundredths of a percent of some petrogenic components. Spinel occurs as lamellae in plagioclases from all samples of type-II rocks and more rarely in *Grt* forming symplectites with *Cpx* (sample 20.3). This symplectite contains not only spinel (point 8), but also corundum (Fig. 2f). Lamellae are fine randomly oriented thin laths 10–60 μm long (Figs. 3b and 4f), but sometimes they show systematic orientation, like corundum (Fig. 2d). Spinel contains 1.5–2 times more FeO than MgO. Composition of *Pl* with spinel inclusion corresponds to oligoclase An 27% (samples 13.1 and 88.1). Sapphirine was found in sample 88.1 as symplectites with *Pl*. The occurrence of sapphirine in retrograde eclogites is usually interpreted as evidence for ascent of deep-seated rocks at high temperature (Sabau et al., 2002). It should be noted that the finds of sapphirine are confined to the objects that experienced complex structural transformations, as well as to the rocks having peculiar features, for instance, positive Eu anomaly (Thomas and Nixon, 1987).

#### *P–T Estimate of the Formation of the Rocks of the Kandalaksha Structure*

*P–T* conditions estimated with TPF software for the Kandalaksha anorthosite massif and garnet–clinopyroxene rocks confined to its upper part were used to construct a metamorphic evolution path of these rocks (Fonarev et al., 2007). This evolution was polymetamorphic with ultrahigh (1000–1040°C) temperature of peak metamorphism at high pressures around 14–15 kb. Most part of garnet was formed at peak conditions and its composition has been preserved in some grains during subsequent prograde processes. The rocks of the Kandalaksha Massif were metamorphosed at higher *P–T* conditions as compared to the Kolvitsa Massif. Three tectonothermal events are recorded. As in other cases (Fonarev, 2004), the evolution of the region represents an alternation of subisobaric cooling and subisothermic decompression. The rocks from the eastern part of the Kandalaksha structure, which are spatially associated with olivine-bearing varieties, yield even higher metamorphic parameters of *T*–900°C and *P*–16.5 kb (Skublov and Terekhov, 2009).

#### *REE Distribution in the Studied Rocks and Minerals*

Data on the REE composition of all rock varieties of the Lapland granulite belt have been reported in (Terekhov and Levitskii, 1993; Skublov, 2005). Mafic granulites are subdivided into two groups (Fig. 6a). One group is characterized by the tholeiitic REE pattern typical of the amphibolite and granulite xenoliths in Archean granite gneisses of the Karelian and Kola cratons (Terekhov and Efremova, 2005). Other, high-Al group, has a differentiated REE pattern with  $(La/Yb)_n = 5–9$ . In terms of REE distribution pattern and other parameters, the high-alumina granulites are similar to the calculated primary composition of layered intrusions and drusites and could be considered as the early phases of the deep-seated crystallization of yet undifferentiated magma of the Paleoproterozoic plume (Sharkov et al., 1997). Unlike the widest spread granulites, all olivine-bearing varieties show low REE abundances, weak fractionation, and positive Eu anomaly (Figs. 6b, 6c). The Eu anomaly is frequently thought to be related to *Pl*, but samples 21.1 and 83.2 contain no plagioclase. The positive Eu anomaly is observed in *Cpx* and *Grt* from sample 83.1 (Fig. 6d) (Skublov and Terekhov, 2009). Such REE distribution in the indicated minerals is rare phenomenon and was noted in the xenoliths in volcanic pipes (Chu Lee et al., 1997). *Grt* with positive Eu anomaly was also found in *Grt*–*2Px* granulite xenoliths in the Devonian volcanic pipe on Elovoy Island in Kandalaksha Bay (Fig. 6f) (Koreshkova et al., 2001). The studies of the REE distribution pattern in the minerals of the Lapland belt show that garnet, clinopyroxene, and amphibole have high REE abundances and the negative Eu anomaly (sample 81.1), even if bulk rock, for instance,



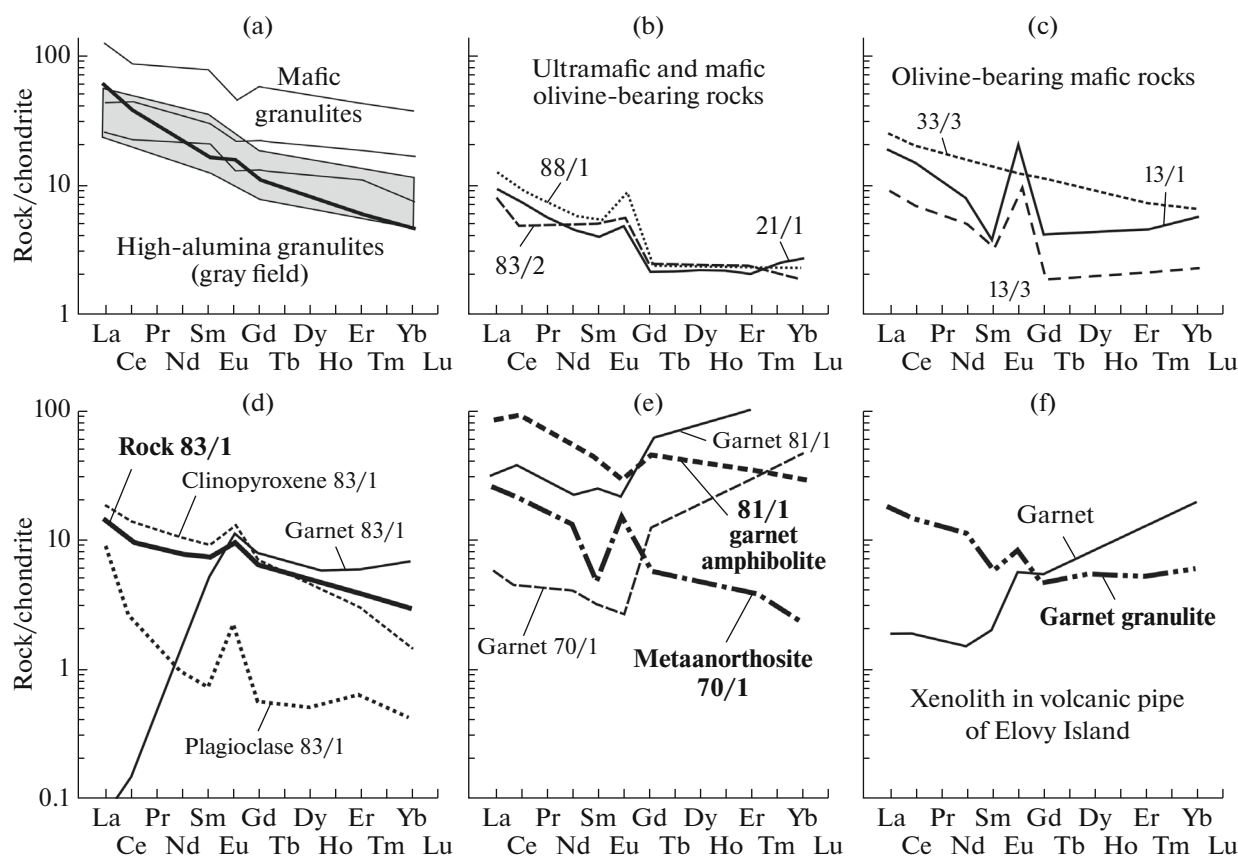


**Fig. 6.** Chondrite-normalized REE contents in the olivine-bearing and associated rocks of the Kandalaksha structure. (a) REE distribution in the representative samples of mafic granulites (moderate-alumina) and field of high-alumina mafic granulites. Bold line shows REE abundance in the inferred melt for drusites and layered intrusions; (b) olivine-bearing ultramafic rocks; (c) olivine-bearing rocks with plagioclase and metaanorthosites; (d–f) rocks and their minerals in different parts of the structure. Data were taken from (Terekhov and Levitsky, 1993; Koreshkova et al., 2001; Skublov and Terekhov, 2007). Normalized after (Nakamura, 1974).

metaanorthosite, has positive Eu anomaly (for instance, metaanorthosite) (sample 70.1). Note that garnets from metaanorthosite and garnet amphibolite have similar REE distribution pattern and the negative Eu anomaly (Fig. 6e), although replaced *Pl* is characterized by the positive Eu anomaly. Thus, the olivine-bearing varieties and their minerals have anomalous REE distribution pattern possibly inherited from compositionally peculiar protoliths or caused by the influence of mantle-derived reduced fluids.

## DISCUSSION

Garnet (pyrope 29.5 mol %, grossular 22.4 mol %)—clinopyroxene inclusion (jadeite 36.9 mol %) pair found in the studied rocks may be regarded as assemblage of the early stage of eclogitization of a magmatic protolith. In sample 88.1, one grain similar in composition to omphacite reveals a prograde zoning (30.5 mol % jadeite in rim and 19.4 mol % in core). There are garnet grains with 40–44 mol % pyrope, 30–35 mol % grossular, and the lowered content of

almandine and spessartine. *Pl* (An 34%) from sample 13.3 contains two omphacite grains (jadeite 33.7 and 36.1 mol %) with prograde zoning and several *Grt* grains, one of which is enriched in grossular and pyrope components but depleted in almandine and spessartine. This *Cpx–Grt* assemblage is also related to the early metamorphic stage, when interaction between olivine and labradorite with participation of diopside resulted in the formation of omphacite and garnet. The characteristic feature of the studied rocks is the coexistence of high-jadeite *Cpx* and low-pyrope *Grt* or, vice versa, relatively low-jadeite *Cpx* and high-pyrope *Grt*. Most of *Grt* grains show weak reverse zoning. Several grains are homogenous and only one grain shows normal zoning and possibly represents a relict mineral. Reverse zoning of *Grt* indicates that it was formed during retrograde metamorphism, while weak zoning or even its absence are indicative of insignificant change in fluid composition. The position of *Grt* data points in the diagram (Fig. 5b) shows that the rocks during ascent suffered eclogite- to amphibolites-

facies metamorphism. Thus, the considered rocks are retrograde altered eclogites.

Orthopyroxene experienced multiple metamorphic transformations, which follows from the variable content of alumina (1.2–4.2%) and its symplectitic intergrowths with *Cpx* and *Pl*. *Opx* in symplectites has elevated FeO and MnO contents, which correspond to relatively low *P–T* conditions. There are also single grains of relict magmatic *Opx* with low content of Al<sub>2</sub>O<sub>3</sub> (less than 1.5 wt %) and high (up to 2 wt %) Cr<sub>2</sub>O<sub>3</sub>. Some minerals in the olivine-bearing rocks are characterized by the elevated contents of Al<sub>2</sub>O<sub>3</sub>, whereas *Opx* shows an opposite trend. The Al<sub>2</sub>O<sub>3</sub> content is usually no more than 4.2%, whereas hypersthene in the mafic granulites from the Lapland Belt contains 5–7%, sometimes up to 11% Al<sub>2</sub>O<sub>3</sub> (Krylova, 1983). The Al<sub>2</sub>O<sub>3</sub> content in hypersthene shows a positive correlation with pressure, increase of which up to 10–11 kb facilitates Al<sub>2</sub>O<sub>3</sub> solubility in the mineral. Further increase of pressure causes an opposite effect (Drugova et al., 1972). The Al<sub>2</sub>O<sub>3</sub> content also decreases with increasing temperature. An increase of pressure and temperature leads to the change of coordination Al<sub>VI</sub>/Al<sub>IV</sub> ratio, which makes aluminum more mobile and causes its removal from hypersthene (Mysen and Boettcher, 1975). Thus, we may suggest that the low Al<sub>2</sub>O<sub>3</sub> in *Opx* may indicate its formation at pressure more than 11 kb.

Of special interest is olivine. There are grains with higher and lower Fe contents. The latter are usually observed as inclusions in *Cpx* and *Opx*. Olivine is usually magmatic in origin, although there are examples of its secondary formation (Peltonen, 1990). The characteristic feature of metamorphic olivine is its high Fe mole fraction (25–40%), which is not typical of olivine from ultramafic–mafic magmatic rocks (Smol'kin et al., 2000). No signs of olivine development after other minerals are observed in the studied polished thin sections. In contrast, the occurrence of fine olivine crystals as inclusions in *Cpx* and *Opx* may indicate its early origin. These inclusions have the lower Fe mole fraction, contain 0.06–0.14 wt % CaO, and possibly represent relicts of magmatic rock. High-Fe olivine is devoid of CaO. In one sample, olivine is in contact with *Grt* containing 50% pyrope molecule and bears traces of deformations, as other minerals. All presented data suggest that the olivine may be considered as relict magmatic mineral. Why is olivine preserved during retrograde processes? The studies by (Bazylev et al., 2003) showed that olivine is more stable than ortho- and clinopyroxenes during high-temperature and retrograde metamorphism.

The studied olivine-bearing rocks may be compared to veined rocks of the Main Range anorthosite massif, which are known as harrisites (Chistyakov and Kudryashova, 2010). The Main Range Massif is correlated with the anorthosite massifs of the Lapland Belt: Kandalaksha, Kolvitsa, and Sal'nye Tundras

(Priyatkina and Sharkov, 1979). However, it differs in the presence of garnet and olivine–plagioclase rocks (troctolites). Olivine in troctolites has magmatic composition (*Fo*<sub>95–80</sub>) (Sharkov and Chistyakov, 2012). But olivine in the harrisites—lenticular small intrusive bodies made up of the troctolite–gabbro-norite series—has essentially different composition (*Fo*<sub>71–68</sub>), which is close to olivine from the studied rocks. Harrisites are characterized by complex morphology and oriented subparallelly to the layering of host anorthosites. They are characterized by the low contents of TiO<sub>2</sub>, Cr, Ni, Co, and REE with positive Eu anomaly. Thus, the olivine-bearing rocks of the Kandalaksha massif are texturally and geochemically similar to harrisites representing the late derivatives of the Main Range intrusion. Therefore, not only the Kandalaksha anorthosite intrusion, but also minor bodies of the olivine-bearing rocks may be derivatives of the Sumian plume.

Geochronological and petrological data obtained by many researchers indicate that the granulite metamorphism in the Lapland Belt started immediately after magmatic crystallization of the gabbroanorthosite intrusions and caused their metamorphism at peak parameters of *P* = 13–14 kb and *T* = 900°C (Fonarev, 2004). Peak metamorphic parameters of *T* = 900°C and *P* = 16.5 kb for the olivine-bearing varieties of the Kandalaksha massif are higher in pressure than those determined for the Kandalaksha–Kolvitsa fragment and the entire Lapland belt and correspond to the eclogite facies conditions. Similar situation is typical of the Belomorian belt, where 2.45 Ga-old gabbro-norite dikes cutting across the amphibolite-facies rocks contain eclogite assemblages (Travin and Kozlova, 2005). The reasons for the selective eclogitization remain controversial but facts indicate the leading role of deformation and related fluid flows during formation of these rocks (Aranovich and Kozlovskii, 2009). The magmatic protoliths of the olivine-bearing rocks were emplaced at the deeper seated levels than the Belomorian dikes. For this reason, the studied rocks have no cross-cutting relations, but the degree of their metamorphism is higher (16.5 kb and 900°C) (Fonarev et al., 2007; Skublov and Terekhov, 2009) than surrounding framework (12–14 kb and up to 900°C) (Fonarev, 2004).

In addition to the high aluminum content in rock-forming minerals, the olivine-bearing rocks contain corundum, spinel, and sapphirine. Spinel and sapphirine occur in symplectites, whereas corundum form well-shaped prismatic crystals, some of them are very thin and may be termed acicular or filamentary. Such comparison is intensified by the presence of axial zone in corundum from sample 33.3 (Fig. 3f). It is known that the grown filamentary crystals often have axial channel. The studies of filamentary crystals, in particular, corundum, show that such morphologies are generated from a gas phase (Berezhkova, 1969).



This indicates a fluid influx of alumina, which is also supported by enrichment in  $\text{Al}_2\text{O}_3$  (up to 14 wt %) of *Cpx* in symplectites with *Grt*, where lowered  $\text{Al}_2\text{O}_3$  should be expected. Many amphibole grains contain up to 19%  $\text{Al}_2\text{O}_3$ . This indicates the contribution of alumina-rich fluid at different stages of regression. The activity of alumina-rich fluid flows in this region is also supported by the presence of high-alumina metasomatites in the Earth's crust sequence initially localized above the Kandalaksha Massif. These are cordierite—sillimanite, kyanite, fuchsite—garnet, and miaceous rocks (Terekhov, 2007).

One of the geochemical characteristics of the Earth's crust composition is the presence of the negative Eu anomaly. With allowance for the fact that the total crust has no Eu anomaly, some researchers suggest the presence of the positive Eu anomaly in the lower crust (Taylor and McLennan, 1985). It is related to the presence of residues remained after extraction of granites that formed upper crust. However, most of the known granulites have no positive Eu anomaly. The maximum positive Eu anomalies were found in felsic granulites, which is inconsistent with the model of granite extraction (Rudnic, 1992). Therefore, the finds of rocks with complementary positive Eu anomaly has remained an urgent problem. Geochemical feature of the studied olivine-bearing rocks is the presence of Eu anomaly in their bulk composition, as well as in garnet and clinopyroxene. It is generally known that REEs are linked to volatiles (Balashov, 1976). The appearance of the positive Eu anomaly could be related to the deep-seated reducing fluids, which extract from the rock such elements as Ti, Cr, Zr, REE, and to lesser extent, Eu. Such mechanism of the formation of the positive Eu anomaly was proposed for veined felsic rocks (Terekhov and Shcherbakova, 2004). Intense fluid reworking related to the formation of eclogites leads to the total REE decrease and the appearance of the positive Eu even in such REE-enriched mineral as zircon (Kaulina et al., 2010; Berezin et al., 2013). In the considered rock complex, the activity of endogenous fluid may be related to the decompression in the rift zone of the Baltic Shield. In the present-day position, this zone includes the Pechenga—Imandra—Varzuga and Karelian trough belts, which in the Paleoproterozoic were localized above the granulite metamorphic zone (rift pillow) (Terekhov, 2007).

Minor bodies of the olivine-bearing rocks in the Kandalaksha structure could be “echo” of the deeper seated and larger scaled phenomena, and their study provides insight into petrogenetic processes at the lithosphere base. Similar rocks presumably compose the root parts of young rift systems, while their volumes should be more, thus increasing their role in the petrochemical differentiation of the Earth's crust. Using the studied olivine-bearing rocks as an example, we may suggest that significant upper mantle volumes

made up of the olivine—pyroxene—garnet rocks, piclogites (after Anderson, 1989), could be formed not only during underplating and emplacement of deep-seated magmas, but also under the effect of fluid-assisted metamorphic processes.

## CONCLUSIONS

The olivine-bearing garnet—pyroxene rocks studied for the first time in the Lapland granulite belt formally may be correlated with piclogites. The study of minerals in these rocks revealed several zoned prograde metamorphosed omphacite grains containing 30–37% jadeite in rims and garnet with 45–50% pyrope. The presence of relict omphacite and garnet suggests that the considered rocks are transformed eclogites.

A wide compositional range of clinopyroxene and garnet, the presence of their grains with normal, reverse, and complex zoning, and the absence of the equally transformed mineral pairs (usually, a combination of high jadeite and low pyrope, or vice versa), indicate a repeated change of  $P$ – $T$  parameters leading to the mineral transformations.

Olivine in the considered rocks possibly represents relict magmatic mineral. Olivine with lower Fe content is observed as inclusion in the clino- and orthopyroxenes and in terms of CaO and Cr contents is close to magmatic minerals. Varieties with higher Fe contents likely suffered high to moderate-temperature metamorphism.

According to geochemical features of the studied rocks and the presence of olivine and coronite textures, the protoliths of the studied rocks could be mafic (olivine gabbro-norite) and ultramafic rocks (websterites), which likely are facies analogues of the gabbroanorthosites of the Lapland Belt.

The olivine-bearing rocks contain corundum, spinel, and sapphirine, as well as have elevated  $\text{Al}_2\text{O}_3$  contents in some clinopyroxenes and amphiboles (13–14 wt % in pyroxene and 17–19 wt % in amphibole). This indicates that the ascent of the deep-seated rocks to the surface was assisted by Al-rich fluid. These fluids presumably extracted from rocks some components, including REE (besides Eu). The reducing character of the fluid is confirmed by the presence of the positive Eu anomaly in the bulk rock composition and in the constituent rock-forming minerals.

Activation of fluid reworking leading to the formation of the olivine-bearing rocks, their transformation, transfer of alumina and its precipitation at different depths are related to the decompression at the base of the Paleoproterozoic rift system of Karelides. Similar processes possibly led to the formation of the deeper seated olivine-bearing eclogites (piclogites).

## ACKNOWLEDGMENTS

This work is the continuation and further development of studies of metamorphism of the Kandalaksha structure, which were carried out by V.I. Fonarev and completed with financial support of the Russian Foundation for Basic Research (project nos. 13-05-298 and 14-05-00149) and the Earth Science Division of the Russian Academy of Sciences (program no. 10).

The summary table of microprobe analyses of the rocks of the Kandalaksha structure is available from authors upon request as application to this paper.

## REFERENCES

- D. L. Anderson, *Theory of the Earth* (Blackwell, Boston, 1989).
- L. Ya. Aranovich, and V. M. Kozlovskii, "The role of silica mobility in the formation of "incipient" eclogites," *Geochem. Int* **47** (2), 199–204 (2009).
- Yu. A. Balashov, *Geochemistry of Rare-Earth Elements* (Nauka, Moscow, 1976) [in Russian].
- G. V. Berezkhova, *Whisker Crystals* (Nauka, Moscow, 1969) [in Russian].
- B. A. Bazylev, S. Karamata, and G. S. Zakariadze, "Petrology and evolution of the Brezovica ultramafic massif, Serbia," *Geol. Soc. London, Sp. Publ.* **218**, 91–108 (2003).
- A. V. Berezin, S. G. Skublov, Yu. B. Marin, A. E. Mel'nik, and E. S. Bogomolov, "New occurrence of eclogite in the Belomorian Mobile Belt: geology, metamorphic conditions, and isotope age," *Dokl. Earth Sci.* **448** (1), 43–53 (2013).
- A. V. Chistyakov, and E. A. Kudryashova, "Harrisites—a final phase of the Monchegorsk mafic–ultramafic complex, Kola Peninsula," *Izv. Vyssh. Ucheb. Zaved. Ser. Geol.*, No. 6, 16–21 (2010).
- V. I. Fonarev, "Metamorphic evolution of the Kolvitsa anorthosite massif (Lapland–Kolvitsa granulite belt, Baltic Shield), *Dokl. Earth Sci.* **395** (3), 364–368 (2004).
- V. I. Fonarev, E. N. Terekhov, and A. N. Konilov, "Ultra-high-temperature—High-Pressure granulite metamorphism of the Kandalaksha Massif (Baltic Shield)," in *Proceedings of 2<sup>nd</sup> All-Russian Conference "Granulite Complexes in the Precambrian and Phanerozoic Geological Evolution, St. Petersburg, Russia, 2007"* (St. Petersburg, 2007), pp. 369–373 [in Russian].
- T. G. Frisch, D. Jackson, V. A. Glebovitsky, M. M. Efimov, M. N. Bogdanova, and R. R. Parrish, "U–Pb geochronology of zircons from the Kolvitsa gabbroanorthosite complex, southern Kola Peninsula, Russia," *Petrologiya* **3** (3), 248–254 (1995).
- G. M. Drugova, V. A. Glebovitskii, L. V. Limov, L. P. Nikitina, and L. A. Priyatkina, *Granulite-Facies Metamorphism* (Nauka, Moscow, 1972) [in Russian].
- T. V. Kaulina, and M. N. Bogdanova, "Main stages in the evolution of the northwestern Belomorian zone: U–Pb data," *Litosfera*, No. **12**, 85–97 (2000).
- T. V. Kaulina, V. O. Yapaskurt, S. L. Presnyakov, E. E. Savchenko, and S. G. Simakin, "Metamorphic evolution of the Archean eclogite-like rocks of the Shirokaya and Uzkaya Salma area (Kola Peninsula): geochemical features of zircon, composition of inclusions, and age," *Geochem. Int.* **48** (9), 871–890 (2010).
- N. E. Kozlov, A. A. Ivanov, and M. I. Nerovich, *Lapland Granulite Belt—Primary Nature and Evolution* (Geol. Inst. Kol. Fil. Akad. Nauk SSSR, Apatity, 1990) [in Russian].
- M. D. Krylova, *Geological—Geochemical Evolution of the Lapland Granulite Complex* (Nauka, Leningrad, 1983) [in Russian].
- M. Yu. Koreshkova, L. K. Levskii, and V. V. Ivanikov, "Petrology of a lower crustal xenolith suite from dikes and explosion pipes of the Kandalaksha Graben," *Petrology* **9** (1), 79–96 (2001).
- M. Marker, "Early Proterozoic (c 2000–1900 Ma) crustal structure of the northeastern Baltic Shield: tectonic division and tectogenesis," *Norsk. Geol. Unders. Bull.* (403), 55–74 (1985).
- M. V. Mintz, V. N. Glaznev, A. N. Konilov, N. M. Kunina, A. B. Raveskii, Yu. N. Sedykh, V. M. Stupak, and V. I. Fonarev, *Early Precambrian of the Northeastern Baltic Shield: Paleogeodynamics, Structure, and Evolution of the Continental Crust* (Nauchnyi Mir, Moscow, 1996) [in Russian].
- F. P. Mitrofanov, and L. I. Nerovich "Timing of magmatic crystallization and metamorphic transformations in the Pырshin and Abvar autonomous anorthosite massifs, Lapland Granulite Belt," *Petrology* **11** (4), 343–351 (2003).
- B. O. Mysen and A. L. Boettcher, "Melting of a hydrous mantle," *J. Petrol.* **16** (3) 549–593 (1975).
- N. Nakamura "Determination of REE, Ba, Fe, Mg, Na and K in carbonaceous and ordinary chondrites," *Geochim. Cosmochim. Acta* **38**, 757–775 (1974).
- P. Peltonen, "Metamorphic olivine in picritic metavolcanics from Southern Finland," *Bull. Geol. Soc. Finland* **62** (2), 99–114 (1990).
- L. L. Perchuk, D. A. Tokarev, D. D. van Reenen, D. A. Varlamov, T. V. Gerya, L. V. Sazonova, V. I. Fel'dman, C. A. Smit, M. C. Brink, and A. A. Bisschoff, "Dynamic and thermal history of the Vredefort explosion structure in the Kaapvaal Craton, South Africa," *Petrology* **10** (5), 395–432 (2002).
- Q. Qi, L. A. Taylor, G. A. Snyder, R. N. Clayton, T. L. Mayeda, and N. V. Sobolev, "Detailed petrology and geochemistry of a rare corundum eclogite xenoliths from Obnazhennaya, Yakutia," *Russ. Geol. Geophys.* **38**, 247–260 (1997).
- R. L. Rudnic, "Restites, Eu anomalies, and lower continental crust," *Geochim. Cosmochim. Acta* **56**, 963–970 (1992).
- G. Sabau, A. Alberico, and E. Negulescu, "Peraluminous sapphirine in retrogressed kyanite-bearing eclogites from South Carpathians: status and implications," *Int. Geol. Rev.* **44** (5), 859–876 (2002).
- E. V. Sharkov and A. V. Chistyakov, "The Early Paleoproterozoic Monchegorsk layered mafite–ultramafite massif in the Kola Peninsula: geology, petrology, and ore potential," *Petrology* **20** (7), 607–639 (2012).
- E. V. Sharkov, V. F. Smolkin, and I. S. Krassivskaya, "Early Proterozoic igneous province of siliceous high-Mg



- boninite-like rocks in the eastern Baltic Shield,” *Petrology* **5** (5), 448–465 (1997).
- S. G. Skublov and E. N. Terekhov, “High-pressure granulites of the Kandalaksha Massif: geochemistry of minerals and metamorphic conditions,” *Dokl. Earth Sci.* **425** (3), 409–414 (2009).
- S. G. Skublov, *Rare-Earth Element Geochemistry of Rock-Forming Metamorphic Minerals* (Nauka, St. Petersburg, 2005) [in Russian].
- V. F. Smolkin, V. V. Borisova, S. A. Svetov, and A. E. Borisov, “Late Archean komatiites of the Ura Bay–Titovka structure, northwestern Kola Region,” *Petrology* **8** (2), 177–199 (2000).
- N. V. Sobolev, “Paragenetic types of garnets,” in *Proceedings on Genetic and Experimental Petrography* (SO AN SSSR, Novosibirsk, 1963) [in Russian].
- S. R. Taylor and S. M. McLennan, *The Continental Crust: its Composition and Evolution* (Blackwell, Oxford, 1988).
- E. N., Terekhov, “Lapland–Belomorian mobile belt as an example of the root zone of the Paleoproterozoic rift system,” *Litosfera*, No. **6**, 15–39 (2007).
- E. N. Terekhov, and L. B. Efremova, “Evolution of REE contents in rocks of the Eastern Baltic Shield as indicators of geodynamic environments,” *Geochem. Int.* **43** (11), 1065–1077 (2005).
- E. N. Terekhov, and V. I. Levitskii, Granulites of the Lapland Belt: rare-earth elements and problems of genesis,” *Izv. Vyssh. Ucheb. Zaved. Geol. Razved.*, No. **5**, 3–17 (1993).
- E. N. Terekhov, and T. F. Shcherbakova, “Genesis of positive Eu anomalies in acid rocks from the eastern Baltic Shield,” *Geochem. Int.* **44** (5), 439–455 (2006).
- C. W. Thomas and P. H. Nixon, “Lower crustal granulite xenoliths in carbonatite volcanoes of the Western Rift of East Africa,” *Mineral. Mag.* **51** (363), 621–633 (1987).
- V. V. Travin, and N. E. Kozlova, “Local shear deformations as a cause of eclogitization: evidence from the Gridino melange zone, Belomorian Mobile Belt,” *Dokl. Earth Sci.* **405A** (9), 1275–1279 (2005).
- O. I. Volodichev, A. I. Slabunov, E. V. Bibikova, A. N. Konilov, and T. I. Kuzenko, “Archean eclogites in the Belomorian Mobile Belt, Baltic Shield,” *Petrology* **12** (6), 540–560 (2004).

*Translated by M. Bogina*